

Immobilization of Monolayers Incorporating Cu Funnel Complexes onto Gold Electrodes. Application to the Selective Electrochemical Recognition of Primary Alkylamines in Water

Gaël De Leener,^{†,‡} Ferdinand Evoung-Evoung,[§] Angélique Lascaux,[†] Jeremy Mertens,^{||} Ana Gabriela Porras-Gutierrez,^{§,#} Nicolas Le Poul,^{*,§} Corinne Lagrost,[⊥] Diana Over,[‡] Yann R. Leroux,[⊥] François Reniers,^{||} Philippe Hapiot,[⊥] Yves Le Mest,[§] Ivan Jabin,^{*,†} and Olivia Reinaud^{*,‡}

[†]Laboratoire de Chimie Organique, Université libre de Bruxelles (ULB), Avenue F. D. Roosevelt 50 CP160/06, B-1050 Brussels, Belgium

[‡]Laboratoire de Chimie et de Biochimie Pharmacologiques et Toxicologiques, Université Paris Descartes, Sorbonne Paris Cité, CNRS UMR 8601, 45 rue des Saints Pères, 75006 Paris, France

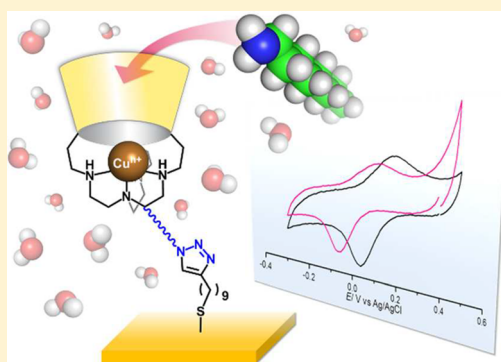
[§]CNRS UMR 6521, Université de Bretagne Occidentale, 6 Avenue Le Gorgeu, CS 93837, 29238 Brest, France

^{||}Chimie Analytique et Chimie des Interfaces, Université libre de Bruxelles (ULB), CP 255, Campus de la Plaine, Boulevard du Triomphe, B-1050 Brussels, Belgium

[⊥]Institut des Sciences Chimiques de Rennes, UMR CNRS 6226, Université de Rennes 1, Campus de Beaulieu, 35042 Rennes, France

Supporting Information

ABSTRACT: The immobilization of a copper calix[6]azacryptand funnel complex on gold-modified electrodes is reported. Two different methodologies are described. One is based on alkyne-terminated thiol self-assembled monolayers. The other relies on the electrografting of a calix[4]arene platform bearing diazonium functionalities at its large rim and carboxylic functions at its small rim, which is post-functionalized with alkyne moieties. In both cases, the CuAAC electroclick methodology proved to be the method of choice for grafting the calix[6]azacryptand onto the monolayers. The surface-immobilized complex was fully characterized by surface spectroscopies and electrochemistry in organic and aqueous solvents. The Cu complex displays a well-defined quasi-reversible system in cyclic voltammetry associated with the Cu(II)/Cu(I) redox process. Remarkably, this redox process triggers a powerful selective detection of primary alkylamines in water at a micromolar level, based on a cavitory recognition process.



INTRODUCTION

Host–guest chemistry at surfaces remains a challenging topic for the development of supramolecular sensors and heterogeneous catalysts. It is also of great interest for the construction of efficient multifunctional devices, which can be controlled and tuned by host–guest interactions.¹ Nature is a vast source of inspiration for such interfacial systems. Molecular recognition in biological media occurs thanks to structural arrangements, which generate beneficial low-range energetic effects (e.g., H-bonding, van der Waals interactions). Hence, a cavity receptor, such as those found in enzymes, can also provide size and shape selection for guest binding. Many synthetic hosting systems based on organic cavities have been designed, offering various shape, size, and chemical composition that can be modulated according to the target objectives. Cyclodextrins, cucurbiturils, and calixarenes have been the most studied in solution and on surfaces for the specific detection of a large panel of metal ions and molecules.² Calixarenes offer several advantages: they have a flexible core prone to induced-fit behavior, and they are

relatively easily functionalizable, being thus tunable for an optimized response toward a defined target guest. Whereas calixarene-based probes for metal ions have been largely investigated,³ fewer examples have been reported for their use as probes for small molecules. Indeed, the development of such probes raises not only problems of selective recognition but also of methods of detection. Grafting electro-active receptors on electrode surface, hence allowing an electrochemical detection, is an appealing strategy. With calixarenes, detection methods based on impedance measurements have been widely used.⁴ Some examples of direct detection of small molecules have been also reported, provided they are themselves electroactive.^{4a,5} For amines, detection of dopamine, tyramine, aniline, and related compounds has been described, but the detection of non-electroactive amines is rare.^{4b,c} The concept proposed in this Article aims at the direct and selective

Received: May 24, 2016

Published: September 4, 2016

detection of non-electroactive amines. The strategy is based on the grafting on an electrode of a Cu funnel complex, whose electrochemical response differs whether or not amines can be coordinated as guest in the cavity.

In a general manner, immobilization of macrocyclic systems has been performed on the basis of the very high affinity of sulfur (thiol, dithiolane, thioether) compounds toward metallic (Au, Ag, Pt) surfaces, resulting in the spontaneous formation of self-assembled monolayers (SAMs).^{3,4b,6} Other strategies, based on photochemical activation of alkene arms for grafting onto silicon,⁷ or hydrophobic interactions between a water-soluble calixarene and reduced graphene oxide, were also developed.^{4a} Among the great number of examples on electrodes or nanoparticles,^{4d,6a,e,8} none has reported so far the combination of a redox-active transition metal with a cavity on a surface. In a related domain, our group has developed the synthesis and spectroscopic/electrochemical studies in solution of calix[6]-arene-based metal complexes. These so-called funnel complexes are mimics of the protein pocket of metallo-enzymes that is connected to the solvent through a hydrophobic corridor participating in the substrate selection.⁹ Their recognition properties toward neutral guest molecules have been largely described. They efficiently associate host–guest interactions and a coordination bond to the metal ion embedded at the bottom of the funnel accessible through the half-open calixarene cone. In particular, among the best guests with divalent transition metal ions are primary amines. They are strongly bound to the funnel complex under various conditions, including organic solvents,¹⁰ water,¹¹ and even micelles.¹² With non-redox-active metal ions, methods of detections such as NMR, isothermal titration calorimetry, or fluorescence are classically used. With a redox-active metal ion such as copper, host–guest behavior can be monitored by electrochemical means. Indeed, with the copper calix[6]arene complexes bearing a tren coordinating cap (calix[6]tren,¹³ see Figure 1),

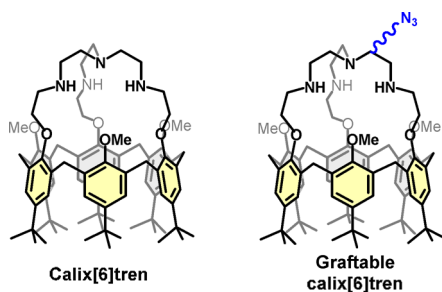


Figure 1. Structures of the calix[6]tren ligand (left) and the targeted ligand (right).

we have evidenced redox-driven mechanisms in organic solution for the guest binding-unbinding processes [acetonitrile (MeCN) vs dimethylformamide (DMF)] depending on the relative affinity of Cu(II) and Cu(I) vs the guest coordinating function.^{9,14} So far, there has been no electrochemical investigation of amine guest exchange for the Cu calix[6]tren complexes. Hence, when immobilized on an electrode, they appeared as promising candidates for amines sensing in organic and aqueous solvents.

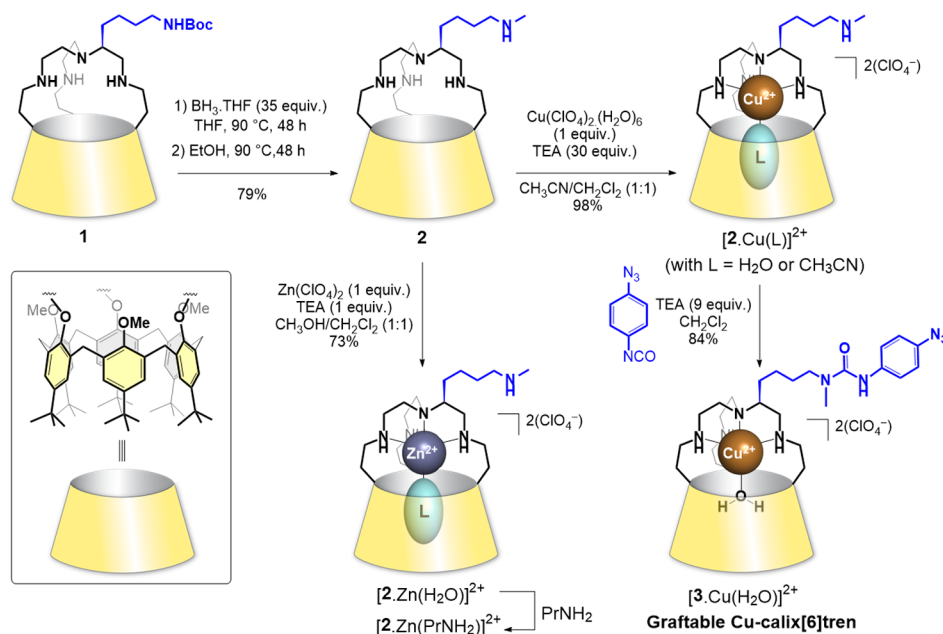
The present study addresses three objectives: (i) synthesis of a calixarene-based ligand bearing a graftable moiety (Figure 1), (ii) immobilization of the corresponding Cu complex as monolayers on an electrode surface, and (iii) exploitation of the

modified electrode by such open-shell Cu cavity complexes for the selective detection of small molecules by direct electrochemical response. Strategies affording monolayers (vs multilayer) were chosen to optimize substrate access and recognition. The “electroclick” approach (Cu-electrocatalyzed azide–alkane cycloaddition, CuAAC) previously developed by our group was specifically used with gold-modified electrodes.¹⁵ The concept is based on the *in situ* activation of the copper catalyst by electrochemical reduction from Cu(II) to Cu(I). It allows monitoring of the grafting by voltammetry if the grafted species contains a redox moiety. It also gives access to the kinetics of immobilization, as previously reported with various copper complexes.^{15b,16,17} Here, the capacities of these modified electrodes to respond to small analytes are illustrated by the selective primary alkylamines detection as a proof of concept since these complexes are prone to display high affinities for such guests. As a matter of fact, primary alkylamines are widely used in a considerable number of industries (e.g., manufacture of dyes and pigments, fuel additives for aerospace and military activities, preparation of coatings, glues, rubbers, polyurethanes, and isothiocyanates, and active pharmaceutical ingredients).¹⁸ However, these amines possess high levels of toxicity for environment and aquatic organisms, as they could be present at low concentrations in water and are considered as potentially carcinogens for human health (important role in food quality control).¹⁹ Given their adverse effects on health and the environment, the development of novel strategies to rapidly, efficiently, and selectively detect primary alkylamines is a challenging task.

RESULTS AND DISCUSSION

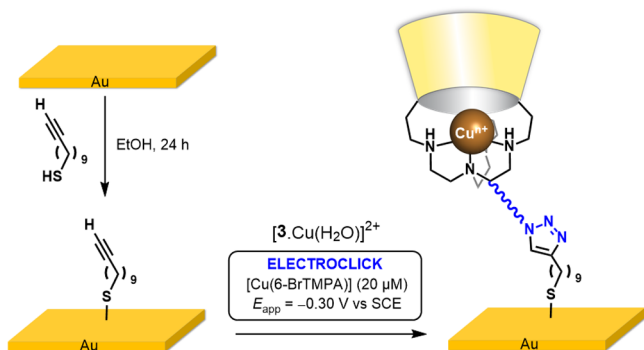
Synthesis and Characterization of Receptors 2 and 3 and Their Zn^{II} and Cu^{II} Complexes. The synthesis of the targeted calix[6]tren ligand required the introduction of an appending graftable arm on the tren unit. To this aim, we used a monofunctionalized calix[6]tren amide precursor (**1**) that was recently reported by some of us (Scheme 1).²⁰ Reduction of the amido and carbamate groups of **1** with BH₃·THF led to the corresponding monofunctionalized calix[6]tren (**2**) in 79% yield. To obtain a derivative that could be grafted through a CuAAC “click” reaction, an azide function was then introduced at the level of the appending arm. For this, protection of the secondary amino groups of the tren moiety was first achieved in 98% yield through formation of the corresponding Cu²⁺ complex, [2·Cu(H₂O)]²⁺. This cupric complex was then reacted with an excess of 1-azido-4-isocyanatobenzene in the presence of triethylamine (TEA), affording the targeted Cu complex [3·Cu(H₂O)]²⁺ in 84% yield. The cupric complexes [2·Cu(L)]²⁺ and [3·Cu(L)]²⁺ were fully characterized by electron paramagnetic resonance (EPR), UV–visible, Fourier-transform infrared (FTIR), and cyclic voltammetry (CV) measurements (see Supporting Information (SI)). In particular, EPR spectroscopy in a frozen dichloromethane (DCM) solution of [2·Cu(H₂O)]²⁺ displayed a rhombic signature that is typical of a Cu complex in distorted trigonal bipyramidal geometry. In order to evaluate the host–guest properties of this new family of calix[6]tren metal complexes by ¹H NMR spectroscopy, the synthesis of the zinc complex [2·Zn(H₂O)]²⁺ was achieved in 73% yield by addition of 1 equiv of Zn(ClO₄)₂(H₂O)₆ to ligand **2**. Similarly to what was observed with the parent calix[6]tren ligand,²¹ further addition of PrNH₂ led to the formation of the complex [2·Zn(PrNH₂)]²⁺, as

Scheme 1. Schematic Pathway for the Syntheses of the Ligands and Complexes



attested by the appearance of high-field shifted resonances belonging to the alkyl chain of the intra-cavity coordinated amine (Figure S3). All these results demonstrate that the presence of an appended arm on the tren cap of receptors 2 and 3 does not affect significantly their metal complexation and hosting properties. Compound $[3.Cu(L)]^{2+}$ appears therefore as a good candidate for studying host–guest interactions involving an immobilized host, in both organic and aqueous environments.

Electroclick Grafting of $[3.Cu(H_2O)]^{2+}$ onto Alkyne-Terminated, Thiol-Modified Gold Electrodes. We have previously developed a two-step electroclick grafting procedure that allows electrochemical monitoring of the grafting of Cu complexes on a pre-functionalized gold electrode.¹⁵ This strategy was used to immobilize the $[3.Cu(H_2O)]^{2+}$ complex onto gold. As a first step, the gold electrode was soaked in an ethanolic solution of undec-10-yne-1-thiol for 24 h (Scheme 2). After thorough washing with absolute ethanol and purified water, the modified electrode was introduced into an aqueous HEPES buffer solution (pH = 9.4) containing 20 μM $[3.Cu(H_2O)]^{2+}$ as well as 20 μM Cu catalyst $[Cu(6\text{-BrTMPA})$

Scheme 2. Strategy for Electroclick Grafting of $[3.Cu(H_2O)]^{2+}$ as Monolayers on Alkyne-Terminated, Thiol-Modified Gold Electrodes

$(H_2O)]^{2+}$ (TMPA = tris(2-pyridylmethyl)amine).¹⁶ The grafting of the Cu-calix[6]tren complex was achieved by cycling 30 times the potential between 0.70 and -0.30 V vs saturated calomel electrode (SCE) with a 3 min hold at -0.30 V between each cycle. The immobilization of $[3.Cu(H_2O)]^{2+}$ was revealed by the appearance of a CV redox process with a gradual increase of the current intensity. After 30 cycles, the intensity of the peaks reached a maximum constant value, suggesting that all accessible “clickable” sites have undergone cycloaddition at the surface (Figure 2A). It was verified by blank procedures that the concomitant presence of both $[3.Cu(H_2O)]^{2+}$ and the catalyst is a prerequisite for the grafting procedure and that there was no pollution of the layer by the electroactive catalyst (Figure S20).

The variation of anodic and cathodic peak currents as a function of time was used to determine the kinetics of the process, assuming that the applied scan rate (0.1 V/s) was fast enough not to perturb the kinetics of grafting. Surface coverage ratio θ (i.e., ratio of time-dependent surface concentration vs maximum surface concentration) was evaluated by peak integration and plotted against time (Figure 2B, red curve). As a first approach, the kinetics were assumed to follow a Langmuir isotherm model (black curve, $n = 1$ see below) based on a pseudo-first-order reaction, as previously done with analogous complexes or ferrocene grafted by electroclick.^{15b,16,22} As shown in Figure 2B ($n = 1$), the simulated curve does not match with the experimental plots ($k = 1.35 \times 10^{-4} \text{ s}^{-1}$). No better fit could be obtained by variation of the k value, which indicates that the grafting process does not follow a classical Langmuir isotherm model. The process started accelerating after 1000 s to finally attain a steady-state regime after ca. 4000 s. Such a change in the kinetic regime was not previously observed for electroclick reactions. Here, the acceleration of the process may be ascribed to positive cooperative effects between the immobilized complexes. To ascertain this hypothesis, a simulation was performed by assuming a JMAK model based on the Avrami equation, which is related to nucleation processes on surfaces:²³

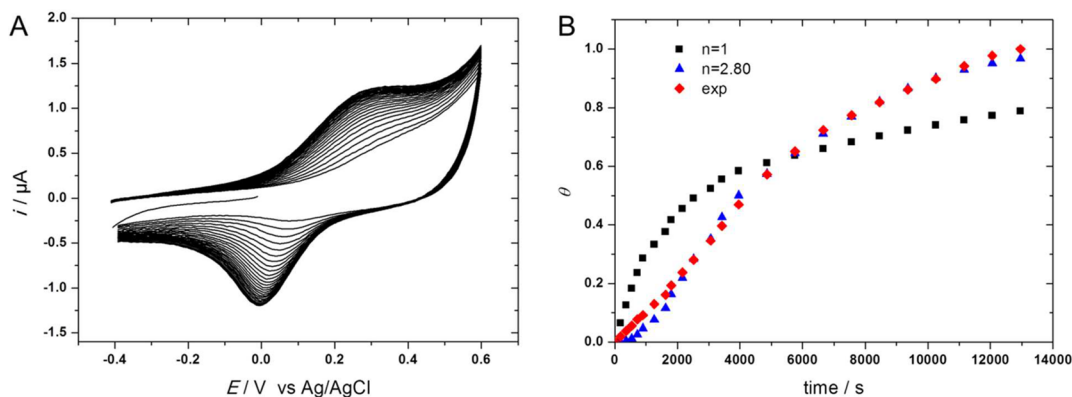


Figure 2. Grafting of $[3\text{-Cu}(\text{H}_2\text{O})]^{2+}$ on an alkyne-terminated, thiol-modified gold electrode under Ar in $\text{H}_2\text{O}/\text{KNO}_3$ 0.1 M + HEPES 0.05 M (pH = 9.4) + $20 \mu\text{M} [\text{Cu}(6\text{-BrTMPA})(\text{H}_2\text{O})]^{2+}$ + $20 \mu\text{M} [3\text{-Cu}(\text{H}_2\text{O})]^{2+}$. (A) Successive CVs during the grafting process ($v = 0.1 \text{ V/s}$, E/V vs Ag/AgCl, 30 cycles). (B) Monitoring of the surface coverage θ as a function of time obtained during the grafting: experimental (red) and simulated plots for $n = 1$ (black) and $n = 2.8$ (blue) with $k = 1.35 \times 10^{-4} \text{ s}^{-1}$.

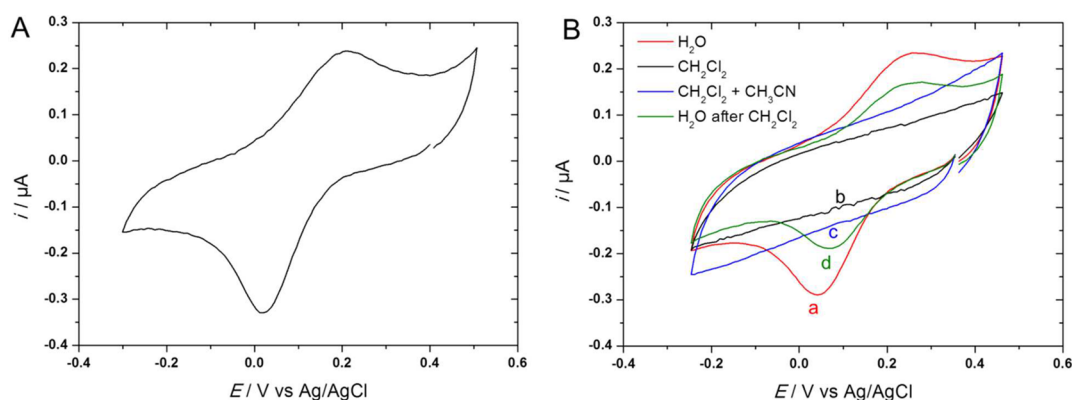


Figure 3. (A) CV ($v = 0.05 \text{ V/s}$) of the grafted Cu-calix[6]tren in $\text{H}_2\text{O}/\text{KNO}_3$ 0.1 M + HEPES 0.05 M (pH = 9.4). (B) Successive CVs ($v = 0.05 \text{ V/s}$) of the grafted Cu-calix[6]tren in (a) $\text{H}_2\text{O}/\text{KNO}_3$ 0.1 M + HEPES 0.05 M (pH = 9.4) (red), (b) $\text{CH}_2\text{Cl}_2/\text{NBu}_4\text{PF}_6$ 0.2 M (black), (c) $\text{CH}_2\text{Cl}_2/\text{CH}_3\text{CN}$ (2% $\text{CH}_3\text{CN} = 250 \text{ mM}$) NBu_4PF_6 0.1 M (blue), and (d) $\text{H}_2\text{O}/\text{KNO}_3$ 0.1 M + HEPES 0.05 M (pH = 9.4) (green).

$$\theta(t) = 1 - \exp[-kt]^n$$

where n is the Avrami number and k the kinetic rate constant.

Hence, for $n = 1$, the model is identical to the Langmuir model (no nucleation). Increase of n induces a distortion of the curve such that the process gently accelerates before attaining a steady-state regime, as usually obtained for chain reactions. As shown in Figure 2B, the best fit with the experimental curve was found for $n = 2.8$ and $k = 1.35 \times 10^{-4} \text{ s}^{-1}$ (blue curve). These data indicate that the grafting of the calix[6]arene complexes occurs preferentially through a nucleation process²⁴ that needs sufficient precursor/catalyst being produced to trigger the reaction. Possibly, immobilization of the first Cu-calix[6]tren complexes on the modified electrode favors the propagation of the electron transfer on the upper side of the monolayer, hence inducing faster kinetics for the click reaction. Additionally, the anchoring of calixarene complexes on the modified surface is assisted by supramolecular interactions (hydrophobic effect) due to first grafted calix[6]tren copper complexes. Notably, the value of k ($1.35 \times 10^{-4} \text{ s}^{-1}$) is significantly lower by 1 order of magnitude than those obtained for grafted ferrocene or small Cu complexes (typically between 2×10^{-3} and $3 \times 10^{-3} \text{ s}^{-1}$).¹⁶ Such a result can be ascribed to steric effects of the calixarene ligand, which slow down the rate of the click reaction on the gold surface.

To ascertain the immobilization of $[3\text{-Cu}(\text{H}_2\text{O})]^{2+}$ on gold as SAMs by electroclick, surface characterization was performed by contact angle measurement, ellipsometry, infrared reflection-absorption spectroscopy, and X-ray photoelectron spectroscopy (XPS). Analysis of the data fully supports the immobilization of the complex on the gold electrode as monolayers (Figures S21–S23).

Voltammetric Studies of Surface-Immobilized Cu-Calix[6]tren in Aqueous Solvents. Electrochemical investigations of the Cu-calix[6]tren-modified surfaces were performed under the same electrolytic and pH conditions that were used for the immobilization process: potassium nitrate 0.1 M with HEPES buffer (pH = 9.4, 0.1 M). As shown in Figure 3A, a quasi-reversible system was detected at $E^0 = 0.11 \text{ V}$ vs Ag/AgCl/NaCl ($\Delta E_p = 190 \text{ mV}$ at $v = 0.1 \text{ V/s}$), which is assigned to the Cu(II)/Cu(I) redox couple. The variation of the scan rate led to an expected increase of both peak current and peak potential separation (Figure S24). However, anodic and cathodic peak intensities do not follow a linear variation with the scan rate as typically observed for immobilized species (Figure S24B). Hence, for $v > 0.1 \text{ V/s}$, the slope of the (i_p vs v) curve is decreasing significantly. In addition, the cathodic and anodic peaks do not show ideal Gaussian shapes as typically obtained with ideal electron-transfer probes such as ferrocenyl derivatives. Such departure from ideality was previously observed for other Cu complexes

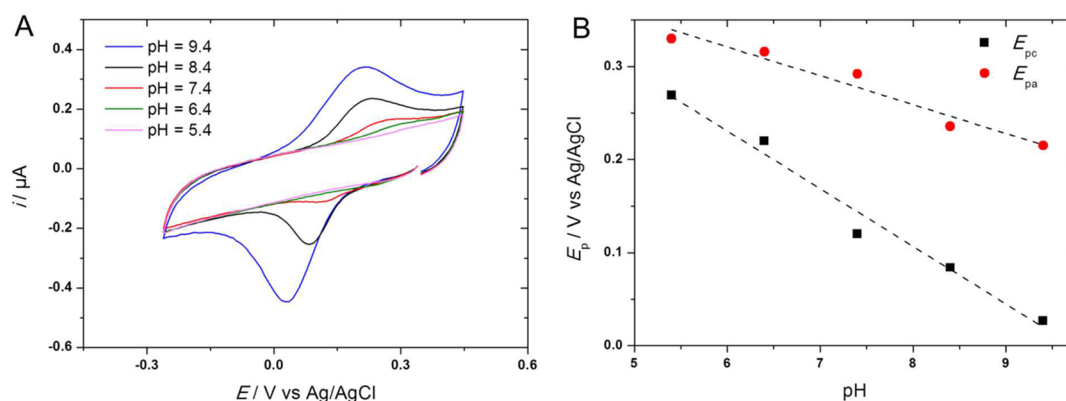


Figure 4. (A) CVs ($\nu = 0.1$ V/s, E/V vs Ag/AgCl) of the grafted Cu-calix[6]tren in H_2O/KNO_3 0.1 M + HEPES buffer 0.1 M at different pH values (decreasing manner: 9.4, 8.4, 7.4, 6.4, 5.4). (B) Plot of E_{pa} (red circles) and E_{pc} (black squares) vs pH.

grafted onto gold-modified electrodes as SAMs.^{15b,16} It is indeed well known that copper complexes often display a non-classic electrochemical behavior because of important geometrical reorganization associated with the Cu(II)/Cu(I) redox system.^{9,25} For the immobilized calixarene complex, these effects can be ascribed essentially to (i) a sluggish electron transfer associated with high reorganizational effects, (ii) lateral interactions between grafted redox centers, which deviate from Langmuir behavior,²⁶ and (iii) a diffusion-like behavior associated with the flexibility of the spacer.¹⁶

The voltammetric behavior of the modified electrode was also investigated in organic solvents. In pure DCM, a total loss of the Cu(II)/Cu(I) faradic process was observed (Figure 3B). Addition of MeCN did not modify the redox response, even in the presence of smaller anions such as chlorides and nitrates. Subsequent soaking and voltammetric studies in aqueous electrolyte restored partially the original signal by ca. 50% (Figure 3B, red and green curves). Such a behavior may arise from copper solvation effects, possibly associated with SAMs disorganization in organic media.²⁷

Experimental surface concentration was determined by integration of the current signal at low scan rates in water ($\Gamma = (1.3 \pm 0.2) \times 10^{-10}$ mol/cm²). The resulting value is approximately 3 times lower than that obtained for a monolayer of ferrocene grafted by CuAAC under similar conditions.¹⁶ Such a result is in agreement with the difference of size between $[3\text{-Cu}(\text{H}_2\text{O})_2]^{2+}$ and the ferrocene derivative, as concluded from XPS analysis. It thus suggests that one single monolayer of Cu-calix[6]tren complex was formed. The redox properties of the immobilized complexes were also investigated as a function of pH. As shown in Figure 4A, the progressive decrease of pH induces a decrease of the peak current intensity as well as a positive shift of the formal potential (ca. 60 mV/decade for E_{pc} , Figure 4B). This indicates that the Cu(II)/Cu(I) electron transfer is coupled to proton exchange (proton-coupled electron transfer, PCET), as previously observed with other copper complexes.²⁸ This is due to the concomitant protonation of a bound ligand (e.g., a hydroxide ion in water) upon reduction of Cu(II). Below pH = 5.4, the peaks of the grafted Cu complex were no longer detected. Hence, at a sufficiently low pH, the tren cap of the ligand can be protonated and Cu(II) is released into the solution, leading to the disappearance of the redox response. This is corroborated by the important decrease of the signal at pH = 9.4 upon soaking into a solution of pH = 5.4 for 30 min (Figure S25B, curve b). Total disappearance was observed after 60 min

(Figure S25B, curve c). Noteworthy, almost all the initial signal was restored at pH = 9.4 by soaking such a de-metalated electrode into a 3 M solution of CuSO_4 ($H_2O/EtOH$, 50:50 v/v) for 24 h (Figure S25A, curve c). This demonstrates that Cu complex de-metalation/re-metalation cycles can be performed with the SAM.

Hence, these electrochemical studies show that the thiol-based grafting procedure leads to a modified surface presenting a good voltammetric response in water of the Cu(II)/Cu(I) process associated with the grafted Cu-calix[6]tren. The next step was to investigate the Cu(II)/Cu(I) response of the immobilized calix complexes to different types of amines as guest ligands by electrochemical means in solution.

Electrochemical Sensing of Alkylamines by SAMs of Cu-Calix[6]tren in Water. Previous studies have shown that calix[6]arene-based tris(imidazole)Zn(II) complexes display remarkable sensing properties toward neutral organic molecules in organic solvents.¹⁰ This is due to the combination of metal coordination, embedded in the heart of the calix cavity, and second coordination sphere effects such as H-bonding between the oxygen lone pairs at the small rim and the bound guest. Selective coordination of primary alkylamines, based on their chemical nature, size, and shape, was evidenced.¹⁰ More recently, a water-soluble version of the ligand that can bind a neutral amine and a zinc cation in an allosteric manner near physiological pH was developed.¹¹ The self-assembly process displayed a remarkable set of biomimetic properties with a spectacular pseudo- pK_a shift of ca. 7 units for the amino guest. Similarly, with the calix[6]tren ligand, recent NMR studies showed that the $[\text{Zn}(\text{calix}[6]\text{tren})(\text{H}_2\text{O})_2]^{2+}$ complex was sensitive and selective toward primary amines in an aqueous environment in the presence of micelles at a millimolar level.¹² The process was interpreted as a guest ligand exchange (water against amine) controlled by the size of the calix[6]arene cone relative to the amine and by specific host-guest supramolecular $\text{CH}-\pi$ interactions. Hence, guest coordination was observed with aliphatic amines such as butyl- or heptylamine, whereas “bulky” amines such as *tert*-butylamine (*t*BuNH₂) did not bind. Aiming at reproducing such effects in aqueous solutions with immobilized Cu complexes, the response of the Cu-calix[6]tren-modified electrode was investigated in electrolytic solutions containing various amines at pH = 9.4. Starting from the aqua copper complex immobilized at the electrode, the addition of non-bulky linear primary amines induced a negative shift of the standard potential E^0 associated with the Cu(II)/Cu(I) process by ca. 100 mV (Figures 5A and S25).

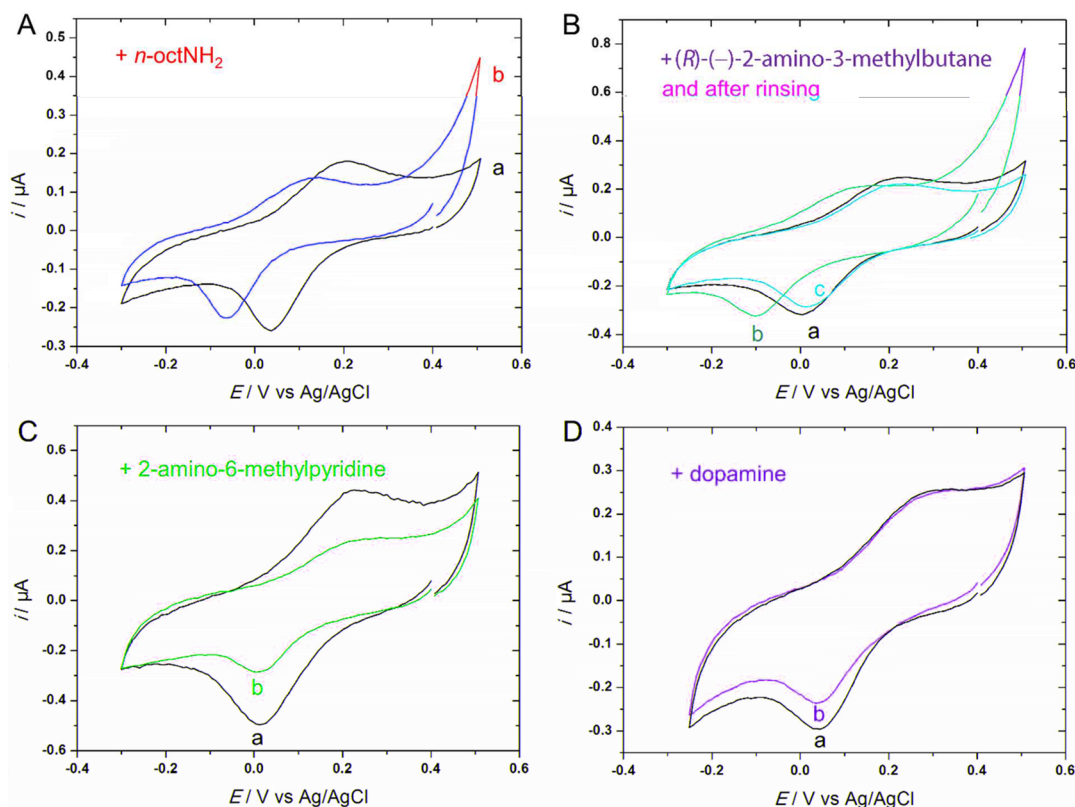


Figure 5. CVs (E/V vs $Ag/AgCl$) of the grafted Cu -calix[6]tren in H_2O/KNO_3 0.1 M + HEPES buffer 0.1 M (pH = 9.4 for A, B, and C; pH = 10.4 for D) before (a, black) and after addition of amine (b, colored): (A) 20 μM n -OctNH₂ (red); (B) 20 μM (R)-(-)-2-amino-3-methylbutane (purple), curve c (cyan), in amine-free solution after rinsing; (C) 50 μM 2-amino-6-methylpyridine (blue); and (D) 50 μM dopamine (orange) (pH = 10.4).

The formal potential E^0 and the peak-to-peak separation were not significantly impacted by the variation of the chain length of the linear amine (propyl, butyl, heptyl, octyl) (Table 1). This

Table 1. Electrochemical Data upon Addition of Amine (20 μM) to the Thiol-Based $[3\cdot Cu(L)]^{2+}$ -Modified Electrode (E/V vs $Ag/AgCl/NaCl$ 3 M) at pH = 9.4

guest	E^0/V	E_{pa}/V	E_{pc}/V	$\Delta E_p/mV$	pKa (H_2O), with ref
no guest	0.11	0.21	0.02	190	—
n -propylamine	0.00	0.10	-0.11	210	10.54 ³²
isopropylamine	-0.01	0.10	-0.12	220	10.63 ³²
n -butylamine	0.00	0.10	-0.10	200	10.60 ³²
(R)-(-)-2-amino-3-methylbutane	0.01	0.12	-0.10	220	10.86 ^{4a}
n -heptylamine	0.03	0.11	-0.05	160	10.67 ³²
n -octylamine	0.03	0.12	-0.06	180	10.65 ³²
N -dansyl-1,6-hexanediamine	0.07	0.17	-0.03	200	10.60 ^{4a}
<i>tert</i> -butylamine	0.11	0.21	0.02	190	10.68 ³²
3-phenylpropylamine	0.11	0.21	0.02	190	10.20 ³³
2-amino-6-methylpyridine	0.11	0.21	0.02	190	7.60 ³⁴
benzylamine	0.11	0.26	0.02	240	9.34 ³²
histamine	0.11	0.21	0.02	190	9.75 ³²
dopamine	0.11	0.21	0.02	190	8.93 ³²
spermine	0.11	0.21	0.02	190	8.83 ³⁵
spermidine	0.11	0.21	0.02	190	8.34 ³⁵

^aCalculated using Advanced Chemistry Development software V11.02 (ACD/Laboratories, 1994–2016).

result falls in line with the similar donor properties of the amines (see pK_a values in Table 1). Interestingly, for all the studied amines, CV of the complex in HEPES solution (pH = 9.4) after rinsing the modified electrode for a few seconds with water (HEPES, pH = 9.4) matched the initial signal with little loss of peak current, as shown in Figure 5B (curve c). This means that amine–water exchange is fully reversible.

The same experiments were then performed with bulkier primary amines, such as isopropylamine (*i*PrNH₂), (R)-(-)-2-amino-3-methylbutane, *tert*-butylamine, and 3-phenylpropylamine (20 μM). For the two first guests, a negative shift of the redox system was detected as in the case of non-bulky and primary alkylamines (Figures 5B and 6A, and Table 1). Conversely, for *t*BuNH₂ and 3-phenylpropylamine, no significant change was observed (Figure S27A,C). This result is in full agreement with those obtained with the analogous Zn complex embedded in micelles (no coordination of *t*BuNH₂).¹² In addition, cyclic and bulkier amines such as benzylamine and 2-amino-6-methylpyridine were also shown to have no effect on the reduction peak potential value (Figures 5C and S26B, respectively), even at higher concentration (2 mM). In most cases, a decrease of the current peak was observed, which may be ascribed to Cu de-metalation and/or SAMs disorganization. The constancy of the redox potential upon addition of these amines can be related to the absence of coordination of the amine to the Cu center, in strong contrast to the primary alkylamines (Scheme 3). Such a selectivity of the redox response of the grafted electrode may be ascribed to two main effects: (i) the size of the calix[6]arene cone that is too narrow to host amines bearing bulky groups in close proximity to the

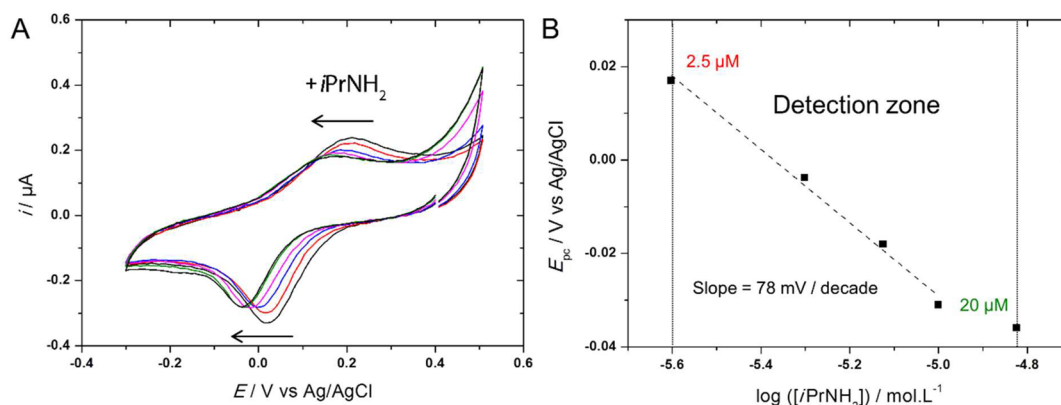
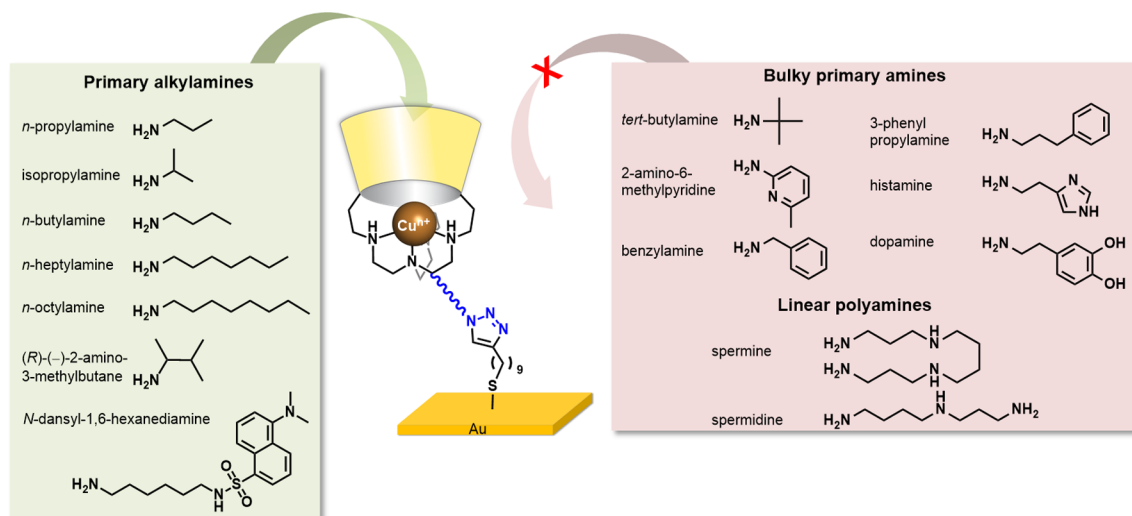


Figure 6. (A) CVs (E/V vs Ag/AgCl) of the grafted Cu -calix[6]tren in $\text{H}_2\text{O}/\text{KNO}_3$ 0.1 M + HEPES buffer 0.1 M ($\text{pH} = 9.4$) upon successive addition of isopropylamine ($0 \mu\text{M}$, $2.5 \mu\text{M}$, $5 \mu\text{M}$, $7.5 \mu\text{M}$, $10 \mu\text{M}$, $20 \mu\text{M}$), (B) Corresponding plot of E_{pc} values vs $\log([i\text{PrNH}_2])$ for $2.5 \mu\text{M} < C < 20 \mu\text{M}$.

Scheme 3. Survey of the Affinities Displayed by the Grafted Cu -Calix[6]tren Complex for Various Guests Presenting a Primary Amino Function, As Measured by CV in Water



amino donor (neither secondary nor tertiary amines),^{10,29} and (ii) the presence of *t*Bu groups at the large rim of the calix[6]arene that form a gate at the entrance of the cavity: the bulkier the guest moiety expanding through the gate, the lower the host–guest affinity, due to the energy cost for its opening.³⁰ Indeed, the electrode remained responsive to a primary amine displaying a long aliphatic chain (hexyl) and a bulky (dansyl) terminal group floating in the solvent outside the cavity, as for linear alkylamines (*N*-dansyl-1,6-hexanediamine, Figure S28).

Competitive binding of primary amines was also investigated by voltammetry. The initial addition of a small alkylamine such as *i*PrNH₂ led to a negative shift of the potential. No modification of the CV was observed upon subsequent addition of other simple alkylamines such as *n*-PrNH₂ and *n*-HeptNH₂ in equimolar amounts (Figure S29A). This is due to the fact that they all give the same electrochemical response at very close potentials (Table 1). Hence, the Cu -modified electrode cannot be used as a sensor to detect a specific amine in the series of small alkylamines. However, this system is of high interest when competing small vs bulky alkylamines in the same solution. Whereas the initial addition of benzylamine did not affect the CV, subsequent addition of an equimolar mixture of *i*PrNH₂ led to the awaited shift of potential, which shows that

the latter is selectively detected in the presence of benzylamine (Figure S29B).

To further investigate the electrode response to amine concentration, we performed progressive addition of *i*PrNH₂ in the 2.5 – $20 \mu\text{M}$ concentration range (buffered solution). CV was characterized by a progressive shift of E^0 (Figure 6A), which follows a linear trend as shown by the plot of E_{pc} against $\log([i\text{PrNH}_2])$ (78 mV/decade , Figure 6B). This redox behavior is typical of a fast and reversible exchange of ligand (amine vs water) associated with the electron-transfer process. It evidences that the calix[6]arene cone (large rim access) is oriented toward the bulk solution on the top side of the SAMs. In addition, minimum and maximum detection limits were evaluated from the CV response: the detection zone ranges from 2.5 to $20 \mu\text{M}$, which is of interest for the development of potentiometric sensors (*vide supra*) (Figure 6).

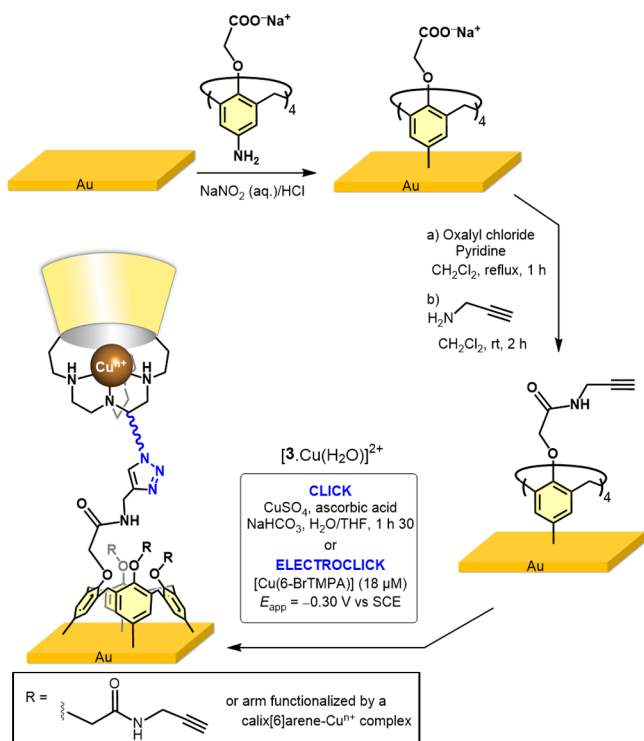
An evaluation of the affinity constants of the grafted copper complexes for the detected alkylamines was obtained from the electrochemical data, assuming a fast ligand exchange mechanism (water against amine) associated with the electron transfer (square scheme).³¹ Fitting of the experimental curves led to a value equal to $5.5(\pm 1) \times 10^5 \text{ M}^{-1}$ at the $\text{Cu}(\text{II})$ redox state for alkylamines displaying large potential shifts, such as

$i\text{PrNH}_2$ (see SI for details, Figure S32). With *N*-dansyl-1,6-hexanediamine, a slightly smaller value ($2.2(\pm 1) \times 10^5 \text{ M}^{-1}$) was found, revealing a small steric hindrance at the level of the *t*Bu substituents of the calixarene large rim (Figure S33).

Electrochemical studies were also carried out with biological relevant amines. For dopamine and histamine, a decrease of the peak current was detected, as observed for synthetic cyclic amines without modification of the reduction peak potential (Figures S2D and S26D, respectively). Increase of the pH until 10.4 for dopamine did not modify the behavior upon addition. With linear polyamines such as spermine or spermidine (Figure S28), no significant change of the redox behavior could be observed. This further illustrates the high selectivity of the recognition process, which makes possible the use of these electrodes for the micromolar detection of alkylamine in the presence of the biological dopamine and analogues (too bulky), as well as polyamines (polyprotonated and too hydrophilic).

Electrochemical Sensing of Alkylamines in Organic Solvents by Cu-Calix[6]tren Grafted on a Calix[4]arene-Modified Electrode. A further challenge was to investigate the possible detection of amines in both aqueous and organic solvents on the basis of the electroclick grafting strategy. Since the redox signal of the copper ion immobilized as thiol-based SAMs disappears in the presence of DCM, we modified the first step (pre-functionalization of the electrode) such that the S–Au bond was replaced by a stronger bond. Hence, on the basis of a recent method,^{36,37} the gold substrate was pre-modified with a calix[4]arene moiety bearing four carboxylate groups at the small rim (Scheme 4). The calix[4]arene platform was electrografted on the gold electrode by reduction of the *in situ*-produced calix[4]arene tetradiazonium salt. As previously demonstrated, a monolayer of calix[4]arene was obtained

Scheme 4. Strategy for Electroclick Grafting of $[3\text{-Cu}(\text{H}_2\text{O})]^{2+}$ as Monolayers on Alkyne-Terminated Calix[4]arene-Modified Gold Electrodes



according to this procedure. The resulting monolayer was further functionalized with propargylamine using acyl chloride activation (Scheme 4).³⁸

Such a procedure allows the functionalization of the gold electrode with covalently attached monolayers terminated by reactive ethynyl arms. The “click” grafting procedure was first evaluated with azido-methylferrocene as a model compound (with copper sulfate and ascorbic acid as reactants). After the grafting process and a thorough washing of the surface, a reversible system that is typical of a ferrocene assembly was observed in EtOH/LiClO₄ 0.1 M ($E_{\text{pc}} = 0.48 \text{ V}$ and $E_{\text{pa}} = 0.52 \text{ V}$ vs Ag/AgCl, $\nu = 0.1 \text{ V/s}$, Figure S30). Plots of i_p vs ν were linear (Figure S30B), indicating the effective immobilization of the Fc molecule on the surface. Surface concentration was evaluated to $\Gamma = 4.4 \times 10^{-10} \text{ mol/cm}^2$, which is a value classically reported for ferrocene monolayers.³⁶ This preliminary result validated our two-step post-functionalization methodology on calix[4]arene-modified electrodes. The next step thus consisted in immobilizing the Cu-calix[6]tren complex on the calix[4]arene platform by both click and electroclick approaches (Scheme 4). The reactions were performed under the same experimental conditions as for azide–methylferrocene. The resulting surfaces were analyzed by CV. In water (pH = 6.8, MES buffer), both click and electroclick approaches display similar results. For electroclick, *in situ* grafting was monitored by CV as shown in Figure 7A. As for the thiol-based procedure, anodic and cathodic peaks appeared upon cycling at 0.2 and -0.1 V , evolving after 10 cycles to 0.0 and -0.15 V respectively, with the appearance of an additional cathodic peak at -0.5 V (Figure 7A). However, these peaks disappeared after washing the modified electrode and successive cycling in an electroactive-free solution, whereas the principal system at 0.1 V remained present. Such a behavior can be inferred to some adsorption of Cu complex on the surface.

After rinsing with water and ethanol, the modified electrodes were studied in both aqueous and organic solvents. In water (pH = 9.1), the voltammetric signal (Figure 7B, curve a, and Figure S31) matched the one obtained with the thiol-SAMs approach with broader peaks. CV experiments were also achieved in different organic solvents. Indeed, as shown in Figure 7B (blue curve), the Cu-calix[6]tren complex grafted on the calix[4]arene platform displayed a low-intensity voltammetric signal in DCM, associated with large peak-to-peak separation: a reduction peak was observed at ca. 0 V vs Ag/AgCl while its oxidation counterpart was located at 1.3 V. This effect is ascribed to the binding/unbinding of water associated with the Cu(II)/Cu(I) redox process.¹⁴ Addition of MeCN induced a drastic negative shift of the oxidation peak potential as a result of the coordination of CH₃CN at the Cu(I) redox state ($E_{\text{pa}} = 0.40 \text{ V}$ vs Ag/AgCl, Figure 7C). Only a small modification of the reduction peak at ca. 0.0 V was observed. These results evidence the detection of a guest (CH₃CN) in organic media by the immobilized copper complex, as found for solution studies (Figure S8). Anodic and cathodic peak potential values for the grafted complex in CH₂Cl₂/CH₃CN (96:4 v/v, $E_{\text{pa}} = 0.40 \text{ V}$, $E_{\text{pc}} = -0.02 \text{ V}$ vs Ag/AgCl), were similar to those found for the free diffusing $[2\text{-Cu}(\text{CH}_3\text{CN})]^{2+}$ complex in similar conditions ($E_{\text{pa}} = 0.52 \text{ V}$, $E_{\text{pc}} = -0.25 \text{ V}$ vs Ag/AgCl, Figure S8). It shows that Cu funnel complexes grafted on the modified surface are little perturbed by electrostatic effects due to their close proximity.

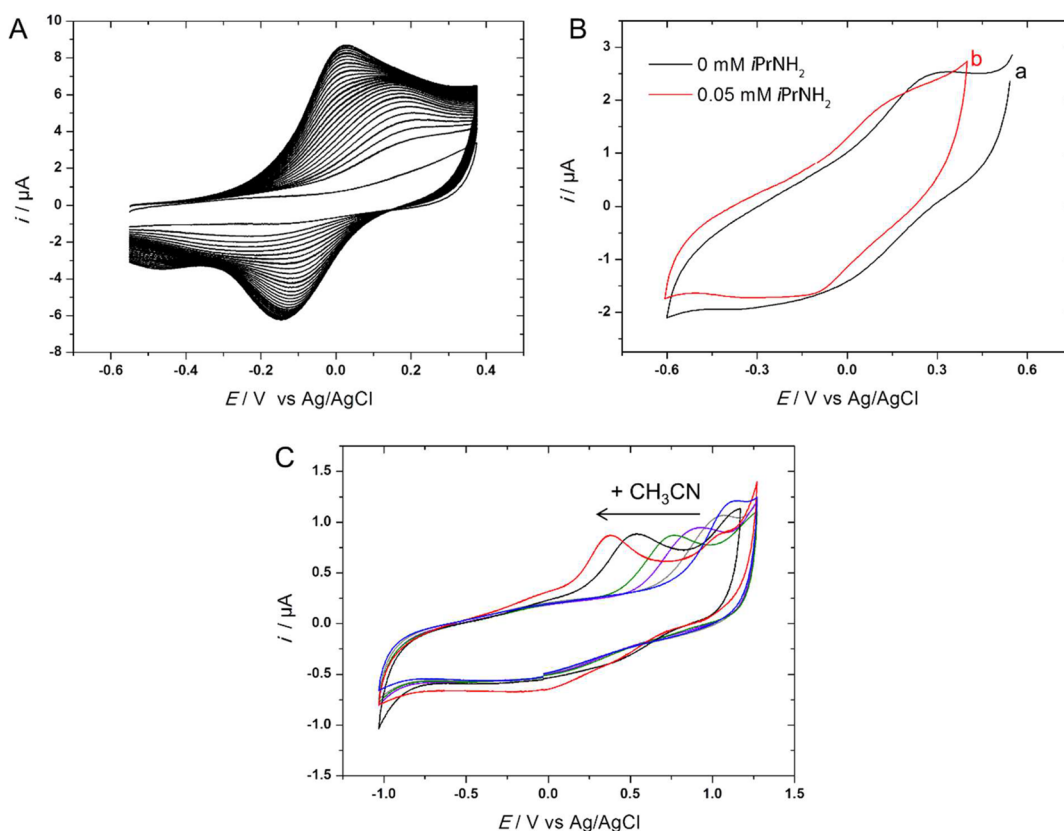


Figure 7. (A) CVs ($\nu = 0.1$ V/s, E/V vs Ag/AgCl, 25 cycles) obtained during the grafting of $[3\text{-Cu}(\text{H}_2\text{O})]^{2+}$ on an alkyne-terminated calix[4]arene-modified gold electrode in $\text{H}_2\text{O}/\text{NBu}_4\text{PF}_6$ 0.1 M + HEPES 0.1 M (pH = 9.2) + $18 \mu\text{M}$ $[\text{Cu}(\text{6-BrTMPA})(\text{H}_2\text{O})]^{2+}$ + $6 \mu\text{M}$ of $[3\text{-Cu}(\text{H}_2\text{O})]^{2+}$. (B) CVs ($\nu = 0.1$ V/s, E/V vs Ag/AgCl) at a Cu-calix[6]tren-grafted calix[4]arene-modified gold electrode in $\text{H}_2\text{O}/\text{KCl}$ 0.1 M + HEPES buffer 0.1 M (pH = 9.1) before (a, black) and after (b, red) addition of 55 mM isopropylamine. (C) CVs ($\nu = 0.1$ V/s, E/V vs Ag/AgCl) in $\text{CH}_2\text{Cl}_2/\text{NBu}_4\text{PF}_6$ 0.2 M at a Cu-calix[6]tren-grafted on calix[4]arene-modified gold electrode upon gradual addition of CH_3CN (blue, before addition; gray, 2.5 mM; purple, 10 mM; green, 60 mM; black, 250 mM; red, 0.8 M (4% vol = 500 mM)).

Amine sensing by the grafted Cu complex was investigated under similar conditions as for the thiol monolayer. As found with thiol-based SAMs, the addition of isopropylamine in a buffered aqueous solution (HEPES 0.1 M, pH = 9.1) induced a negative shift of the redox system by ca. 120 mV (Figure 7B, curve b) but with a much broader response. This value is similar to those found with the thiol system (Table 1) and demonstrates that amine sensing is not affected by the nature of the grafted alkyne-based system (thiol or calix[4]arene).

CONCLUSION

The work described herein relates an original strategy aimed at obtaining electrochemical probes for small molecules. The idea was to use a supramolecular system previously developed, namely a *funnel complex* based on calix[6]arene as a molecular receptor, and to connect it to an electrode that is used as a detector device. For this, a monolayer grafted on a gold electrode was targeted, in order to optimize the access of the analytes to the metal center through the calix funnel. Hence, three key points for this strategy have been validated in this work:

- (i) A calix[6]tren ligand bearing an anchoring arm at the level of the small rim of the conic cavity was successfully synthesized.
- (ii) It was covalently grafted on gold electrodes modified by a monolayer terminated by alkyne moieties. For this purpose the electroclick CuAAC procedure previously

described by us was efficiently used. Two different monolayers were tested. One is a classical SAM obtained with alkyne-terminated thiols. The other exploits a recent methodology based on the covalent electrografting of a calix[4]arene platform that is then post-functionalized with alkyne-terminated arms at its small rim. In both cases, electro-detection of copper bound to the immobilized tren cap was evidenced.

- (iii) The corresponding quasi-reversible Cu(II)/Cu(I) system, as detected by CV, proved to be sensitive to guest ligands. Whereas the thiol-based monolayer was responsive only in water, the calix[4]arene-based monolayer was responsive in both aqueous and organic solvents.

The open-shell cavity property of the Cu complexes on the modified electrodes was exploited for the selective electrochemical detection of alkylamines as a proof of concept. Control of the amine-Cu(II) coordination by the calix[6]arene cavity was demonstrated by voltammetry. Selective detection of amines was obtained at micromolar concentration. The electrochemical response is characterized by a 100 mV shift of the Cu(II)/Cu(I) redox potential in the presence of an amine that is coordinated to the metal center through the calix[6] funnel. The system displayed the selectivity expected for a funnel complex.^{10,29,39} It relies on the donor ability of the guest ligand (amines are excellent donors) and on the shape complementarity between the conic macrocyclic receptor and

the guest: selective primary amine binding (over secondary and tertiary) due to the narrowness of the small rim at which the *N*-donor is coordinated, narrow alkyl moieties in the cone, whereas large substituents floating outside the calix[6]arene are tolerated. It is important to note that the detection through the copper center allows a response of non-electroactive amines, which has been scarcely reported in the literature. Also interestingly, it is shown that the calix[4]arene monolayer is effective in both aqueous and organic media and could be used for the detection of MeCN (below 1% v/v) in a non-coordinating solvent (i.e., non-competitive for an interaction with the metal center).

Hence, this study shows that our strategy is very promising for obtaining a device sensitive to a variety of neutral molecules. Indeed, the grafting methodology of the receptor is relatively straightforward, efficient, and easy to implement. The receptor is highly tunable:⁴⁰ other nitrogenous caps have been shown to confer very different hosting properties to the copper complexes,⁴¹ other metal ions will give different affinities,⁴² and methodologies allowing to introduce various functionalities at the calix[6]arene large rim give rise to multitopic recognition.⁴³ Also, since the recognition pattern is based on the embedded part of the analytes, molecules bearing large groups can potentially be recognized, as long as their bulky substituent stands outside the cavity. Hence large biological molecules may be targeted provided they are functionalized by a spacer arm equipped with a terminal primary amino function.

At last, the strategy developed here opens the way to the immobilization of many other supramolecular systems that incorporate redox-active metals for sensing and catalysis purposes.

EXPERIMENTAL SECTION

Materials and Methods. Most of the reactions were performed under an inert atmosphere. Anhydrous CHCl_3 , CH_2Cl_2 , CH_3CN , and CH_3OH were obtained commercially or distilled from CaH_2 (CHCl_3 , CH_2Cl_2) or P_2O_5 (CH_3CN , CH_3OH) under an inert atmosphere. Anhydrous DMF was obtained commercially or through distillation over a mixture of MgSO_4 , 4 Å molecular sieves and silica gel under argon. Anhydrous THF was obtained from distillation on Na/benzophenone. Water was purified with a filtration system (resistivity = 18.2 $\text{M}\Omega\cdot\text{cm}$). All the solvents and reagents for the syntheses were at least reagent-grade quality and were used without further purification. The reagents and solvents used for surface chemistry were of high-purity grade.

^1H NMR spectra were recorded at 300 or 600 MHz. ^{13}C NMR spectra showed poor signal-to-noise ratio because of the asymmetric functionalization pattern of the compounds and thus cannot be described. The chemical shifts are expressed in ppm, and traces of residual solvents were used as internal standard. CDCl_3 was filtered through a short column of basic alumina to remove traces of DCl. Most of the ^1H NMR spectra signals were assigned on the basis of 2D NMR analyses (COSY, HSQC, HMB). NMR spectra were recorded at 298 K unless otherwise stated. Chemical shifts are quoted on the δ scale, coupling constants (J) are expressed in hertz (Hz). Multiplicity of signals are given by the following abbreviations: s (singlet), d (doublet), t (triplet), q (quadruplet), dd (doublet of doublet), m (multiplet), and b (broad signal).

The EPR spectra were recorded on a X band EPR spectrometer (9.4 GHz, 100 K).

ESI-HRMS analyses were performed using methanol as a solvent. High resolution mass spectra were recorded with an ESI-MS spectrometer equipped with an orbitrap or with a TOF spectrometer.

FTIR spectra were recorded on a potassium bromide window or a FTIR spectrometer equipped with an attenuated total reflectance unit (germanium crystal). Infrared reflection-absorption spectra were

recorded with an infrared incident beam at a 75° angle from the normal to the surface. A total of 500 scans were collected and averaged at 1 cm^{-1} resolution.

The UV-visible spectra were recorded in quartz cells with an optical path of 1 cm.

Specific optical rotations were measured on an automatic polarimeter and were based on the equation $[\alpha] = 100\alpha_{\text{read}}/lC$, where the concentration C is in g/100 mL and the path length l is in decimeters. The units of specific rotation, $(\text{deg}\cdot\text{mL})/(\text{g}\cdot\text{dm})$, and the units of concentration are implicit and are not included in the reported value.

Cyclic voltammograms were recorded with an electrochemical analyzer in a three-electrode setup with an Ag/AgCl/NaCl 3 M ($E = -0.02\text{ V}$ vs SCE, aqueous media) or an Fc/Fc⁺ (organic media) reference electrode and a platinum foil or electrode as counter electrode. All potentials were recalibrated vs Ag/AgCl/NaCl 3 M ($E_{\text{Fc}^+/\text{Fc}} = +0.43\text{ V}$ vs Ag/AgCl).

XPS spectra were acquired using a Mg K α X-ray source ($h\nu = 1253.6\text{ eV}$) operating at 200 W with a 45° takeoff angle (TOA). Here the photoelectron TOA is defined as the angle between the surface normal and the axis of the analyzer lens. Survey spectra (0–1000 eV) were acquired with an analyzer pass energy of 187.85 eV (100 ms time/step, 0.05 s; 0.8 eV/step; six scans); zooms on the Cu 2p and S 2p regions were performed by the accumulation of 30 scans at a 187.85 eV pass energy at 0.4 eV/step with a 300 ms dwell time; high-resolution spectrum of the N 1s core level was acquired at 46.95 eV of pass energy (dwell time; 0.3 s; 0.2 eV/step; 30 scans). Binding energies were referenced to the Au 4f_{7/2} peak at 84.0 eV. The relative atomic concentration for surface composition was calculated using the integrated peaks areas; the peaks area were normalized by the manufacturer-supplied sensitivity factor (Au 4f_{7/2}, 1.9; S 2p, 0.35; C 1s, 0.205; N 1s, 0.38; O 1s, 0.63; Cu 2p_{3/2}, 4.3). The composition was calculated using the average value of three measurements on individual spots for each sample. The core level N 1s spectra were peak-fitted using an adapted software.

Contact angle measurements were performed on an easy drop goniometer equipped with a camera by using a sessile drop method (2 μL of ultrapure water drops). Contact angles were calculated over an average of five measurements. They were determined using a tangent or circle fitting model.

Monolayers thicknesses were estimated by ellipsometry. The polarization angles Ψ and Δ were recorded in the 380–900 nm wavelength range at different incident angles of 65.70 and 75° . The optical constants were fitted with the following values taken for bare gold: $n_s = 0.203$, $k_s = 3.43$. The thicknesses for the organic layer were estimated from a Cauchy model by assuming $n = 1.50$ (refraction index) and $k = 0$ (extinction coefficient).

Caution!

- Although we have not encountered any problem, it is noted that small azide derivatives and perchlorate salts of metal complexes with organic ligands are potentially explosive and should be handled with appropriate precautions.
- The use of phosgene and triphosgene necessitates a particular attention due to the high toxicity of phosgene (gaseous).

Electrode Modification. 1. Thiol-Alkyne Self-Assembled Monolayers. SAMs Preparation. A commercial gold removable tip electrode was used. Before modification, the surface of the gold electrode ($A = 0.07\text{ cm}^2$) was prepared following a classical procedure: after being polished with an alumina (1 μm) slurry, the electrode was sonicated in water and cycled between 0.5 and 1.4 V vs SCE in H_2SO_4 0.1 M (40 scans) to remove gold oxide, washed with water then ethanol, and dried under a slight flow of N_2 before being introduced into the solution containing the thiol derivative. The electrode was kept in a non-mixed undec-10-yne-1-thiol 1 mM solution (solvent: EtOH) for 12 h under N_2 . After thorough washing with pure EtOH, the electrode was stocked in distilled water.

Electroclick Procedure. Grafting of the $[\text{3-Cu}(\text{H}_2\text{O})]^{2+}$ complex onto modified gold electrodes was performed according to a previously published procedure:¹⁶ the electrode was dipped in an

aqueous HEPES buffer solution (pH = 9.4) containing 20 μM $[\text{3-Cu}(\text{H}_2\text{O})]^{2+}$ (previously dissolved in acetone in millimolar concentration) as well as 20 μM Cu catalyst $[\text{Cu}(\text{6-BrTMPA})(\text{H}_2\text{O})]^{2+}$. The grafting of the complexes was achieved *in situ* by cycling the potential 30 times between 0.70 and -0.40 V vs SCE with a 3 min hold at -0.40 V between each cycle.

2. Calix[4]arene Monolayers. Gold substrates were commercial disk electrodes of 3 mm diameter. They were thoroughly polished successively with 5 μm SiC paper, then 1 μm diamond paste on a DP-Nap paper (Struers), and finished with 1 μm DP-Nap paper (Struers) with a 0.3 μm Al_2O_3 slurry.

Surface modification by electrochemical reduction of *in situ*-generated diazonium cations and activation of the carboxylic acid function were performed using already published methodologies.^{36,38}

Functionalization of the Surface with Propargylamine. The system was placed in ice bath. Then a CH_2Cl_2 solution (20 mL) of 6 mmol L^{-1} propargylamine (7.7 μL) was introduced under argon atmosphere with an excess of TEA (30 mM, 16 μL , 5 equiv). After 5 min of stirring in the ice bath, the system was allowed to react at room temperature for 3.25 h. After reaction, the electrodes were immersed into CH_3OH to quench the non-reacted functions on the surface and rinsed with CH_3OH and CH_2Cl_2 .

Click Chemistry Procedure. In a glovebox, three electrodes (gold) were soaked in 2.5 mL of freshly distilled and deaerated THF containing $[\text{3-Cu}(\text{H}_2\text{O})]^{2+}$ (4.5 mg, 9 mM). Next, 1.25 mL of a deaerated aqueous solution of copper sulfate (16 mM) and 1.25 mL of a deaerated aqueous mixture of ascorbic acid (23 mM) and sodium hydrogencarbonate (95 mM) were added. The turbid dark yellow reaction mixture was agitated at room temperature for 1.5 h. The electrodes were then washed in THF under agitation in the glovebox for 1 h. In order to oxidize Cu(I) reduced during the CuAAC reaction, the electrodes were plunged into a freshly distilled and deaerated $\text{CH}_2\text{Cl}_2/\text{NBu}_4\text{PF}_6$ (0.2 M) solution in the glovebox, and a +1 V potential was applied during 5 min.

Electroclick Procedure. Under an inert atmosphere, $[\text{3-Cu}(\text{H}_2\text{O})]^{2+}$ was dissolved in $\text{H}_2\text{O}/\text{KNO}_3$ 0.1 M/HEPES 0.1 M (pH 9.5–10) starting from a stock solution in THF (1 mM, 24 μL). The catalyst $[\text{Cu}^{\text{II}}(\text{6-BrTMPA})(\text{H}_2\text{O})]^{2+}$ was added (72 μL) from a stock solution in acetone (0.01 M, final concentration = 18 μM). A -0.50 V potential (vs Ag/AgCl) was applied during 3 min, and CV was then measured. This cycle was repeated until the intensity of the grafting curve did not increase anymore. The electrode was thoroughly washed with water under an inert atmosphere before analysis (pH 9.5).

Synthesis and Characterization of Compounds. Compound 1 and *N*-dansyl-1,6-hexanediamine were prepared according to procedures previously described in the literature.^{20,44} All reactions were conducted under an inert atmosphere.

Compound 2. In a sealed reactor, $\text{BH}_3 \cdot \text{THF}$ (4.45 mL, 1 M, 4.46 mmol) was added at 0 $^\circ\text{C}$ to a solution of the calix[6]trenamide 1 (185 mg, 0.127 mmol) in THF (5 mL). After the effervescence had stopped, the reaction mixture was heated at 90 $^\circ\text{C}$ for 48 h and then cooled to 0 $^\circ\text{C}$, and ethanol was added dropwise until the effervescence ceased. The reaction mixture was concentrated under reduced pressure, and the residue was dissolved in ethanol (10 mL) and heated at 90 $^\circ\text{C}$ for 48 h. The ethanol was evaporated under reduced pressure, and the residue was heated at 50 $^\circ\text{C}$ under high vacuum for 5 h. The obtained solid was dissolved in CH_2Cl_2 (25 mL) and washed vigorously with an aqueous solution of NaOH (1 M, 10 mL) for 1 h. The aqueous layer was extracted with CH_2Cl_2 (2 \times 10 mL), and the combined organic layers were washed with water (2 \times 20 mL) and then concentrated under reduced pressure. The crude residue was triturated with CH_3CN , and the resulting white precipitate was isolated by centrifugation to give the calix[6]tren 2 (133.0 mg, 79%). mp 240 $^\circ\text{C}$ (dec.); $[\alpha]_D^{20} = +21.1$ ($c = 0.96$, CHCl_3); IR (KBr): $\nu = 2962, 1482, 1460, 1362, 1202, 1120$ cm^{-1} ; the NMR analysis of 2 was done in the presence of imidazolidin-2-one (Imi) and TFA: ^1H NMR of $[\text{2-}n\text{H}\text{Imi}]^{n+}$ (600 MHz, CDCl_3 , 298 K): δ_{H} (ppm) 0.23 (s_{b} , 2H, Imi_{in}), 0.30 (s_{b} , 2H, Imi_{in}), 0.74 (s_{b} , 27H, *t*Bu), 1.32–1.85 (m, 35H, *t*Bu + $\text{CH}_2\text{CH}_2\text{CH}_2\text{CH}_2\text{NHCH}_3$), 2.81 (s_{b} , 3H, NHCH_3), 2.93–3.65 (m, 17H, NCH_2 + NCH + CH_2NH + ArCH_2), 3.87 (m, 9H,

OCH_3), 4.04–4.50 (m, 18H, CH_2NH + OCH_2 + ArCH_2), 4.78 (s_{b} , 1H, NHImi_{in}), 4.79 (s_{b} , 1H, NHImi_{in}), 6.45–6.52 (m, 3H, *ArH*), 6.70 (s, 3H, *ArH*), 7.24–7.33 (m, 3H, *ArH*), 7.39 (s, 3H, *ArH*), 9.92–10.14 (m, 3H, ^+NH); HRMS (ESI-TOF) calculated for $\text{C}_{86}\text{H}_{126}\text{N}_5\text{O}_6$ $[\text{M} + \text{H}]^+$: 1324.9708; measured: 1324.9709.

Compound $[\text{2-Zn}(\text{H}_2\text{O})]^{2+}$. To a solution containing calix[6]tren 2 (10.0 mg, 0.0076 mmol) in distilled CH_2Cl_2 (0.5 mL) was added a solution of $\text{Zn}(\text{ClO}_4)_2(\text{H}_2\text{O})_6$ (2.81 mg, 0.0076 mmol) dissolved in anhydrous CH_3OH (0.5 mL) and TEA (1.02 μL , 0.0076 mmol). The reaction mixture was stirred at room temperature for 1 h. After concentration to a third of the volume by bubbling argon through the solution, a precipitate was obtained. It was separated from the solvent by centrifugation, washed with cold CH_3OH , and dried under vacuum to give $[\text{2-Zn}(\text{H}_2\text{O})](\text{ClO}_4)_2$ (8.8 mg, 73%) as a white solid. IR (NaCl): $\nu = 2964, 2873, 1480, 1363, 1199, 1109, 625$ cm^{-1} ; ^1H NMR (600 MHz, $\text{CD}_3\text{CN}/\text{CDCl}_3$ 1:1, 298 K) δ_{H} (ppm): 0.63–0.79 (m, 27H, *t*Bu), 1.28–1.90 (m, 35H, *t*Bu + $\text{CH}_2\text{CH}_2\text{CH}_2\text{CH}_2\text{NHCH}_3$), 2.53–2.88 (m, 3H, NHCH_3), 2.88–3.75 (m, 17H, NCH_2 + NCH + CH_2NH + ArCH_2), 3.76–3.96 (m, 9H, OCH_3), 4.00–4.66 (m, 18H, CH_2NH + ArCH_2 + CH_2O), 6.20–6.74 (m, 6H, *ArH*), 7.11–7.43 (m, 6H, *ArH*); HRMS (ESI-TOF) calculated for $\text{C}_{86}\text{H}_{126}\text{N}_5\text{O}_6\text{Zn}$ $[\text{M} + \text{H}]^{3+}$: 462.9661; measured: 462.9651.

Compound $[\text{2-Cu}(\text{H}_2\text{O})]^{2+}$. Dry MeCN (1.5 mL) containing $\text{Cu}(\text{ClO}_4)_2(\text{H}_2\text{O})_6$ (14.0 mg, 0.038 mmol) was added to calix[6]tren 2 (50.1 mg, 0.038 mmol) in CH_2Cl_2 (2.5 mL). The reaction mixture was stirred at room temperature for 2 h. After removal of the solvents under reduced pressure, the green solid was re-dissolved in CH_2Cl_2 (3 mL), and the solution was filtered through Celite before removal of the solvent to yield pure $[\text{2-Cu}(\text{H}_2\text{O})](\text{ClO}_4)_2$ as a green powder (64.1 mg, 98%). IR (KBr): $\nu = 2961, 1482, 1362, 1202, 1108, 623$ cm^{-1} ; HRMS (ESI-Orbitrap) calculated for $\text{C}_{86}\text{H}_{125}\text{CuN}_5\text{O}_6$ $[\text{M}]^{2+}$: 693.4463; measured: 693.4415.

1-Azido-4-isocyanatobenzene. The synthesis of this compound was previously reported in the literature, but with another synthetic strategy.⁴⁵

In a reactor, 4-azidoaniline hydrochloride (0.410 g, 2.40 mmol) was dissolved in anhydrous THF (16 mL). Triphosgene (0.713 g, 2.403 mmol) was dissolved in anhydrous THF (16 mL) and injected into the reactor. Freshly distilled TEA (2.92 mL, 21.63 mmol) was then added in one portion. A white smoke was immediately formed (gaseous phosgene). The reactor was sealed and the solution vigorously agitated at room temperature for 19 h. The excess of phosgene was removed by argon bubbling into the solution, and the mixture was concentrated under reduced pressure. The crude residue was rapidly filtered, and the solid was washed with anhydrous THF. The solvent was removed under reduced pressure to afford 1-azido-4-isocyanatobenzene as a brown oil (quant.) that was used without further purification. IR (KBr): $\nu = 3054, 2982, 2259, 2103$ cm^{-1} ; ^1H NMR (300 MHz, CDCl_3 , 298 K): δ_{H} (ppm) 7.08 (d, $J = 9$ Hz, 2H, *ArH*), 6.97 (d, $J = 9$ Hz, 2H, *ArH*).

Compound $[\text{3-Cu}(\text{H}_2\text{O})]^{2+}$. 1-Azido-4-isocyanatobenzene (18.8 mg, 0.117 mmol) was dissolved in anhydrous CH_2Cl_2 (0.5 mL). $[\text{2-Cu}(\text{H}_2\text{O})](\text{ClO}_4)_2$ (23.6 mg, 0.015 mmol) was dissolved in anhydrous CH_2Cl_2 (0.5 mL) and added dropwise to the solution containing the isocyanate. Anhydrous TEA (10 μL , 0.074 mmol) was added, and the mixture was agitated at room temperature. After 17 h, the reaction mixture was washed with water (1 mL) for 15 min. The organic layer was evaporated under reduced pressure, and the crude residue was centrifuged in cold CH_3CN (3 \times 1 mL). The filtrate was concentrated under reduced pressure to afford calix[6]tren $[\text{3-Cu}(\text{H}_2\text{O})](\text{ClO}_4)_2$ as a green-brown solid (84%, 21.8 mg). IR (KBr): $\nu = 3287, 2962, 2115, 1504, 1481, 1362, 1201, 1106, 624$ cm^{-1} ; HRMS (ESI-Orbitrap) calculated for $\text{C}_{93}\text{H}_{129}\text{CuN}_9\text{O}_7$ $[\text{M}]^{2+}$: 773.9666; measured: 773.9640.

■ ASSOCIATED CONTENT

Supporting Information

The Supporting Information is available free of charge on the ACS Publications website at DOI: 10.1021/jacs.6b05317.

Figures S1–S34 and Table S1, giving 1D and 2D NMR spectra of all new organic compounds and NMR host–guest studies of compounds **2** and $[2\cdot\text{Zn}(\text{L})]^{2+}$; EPR, UV–vis, and CV experiments of $[2\cdot\text{Cu}(\text{L})]^{2+}$ and $[3\cdot\text{Cu}(\text{L})]^{2+}$; calculation of thermodynamic constants (PDF)

AUTHOR INFORMATION

Corresponding Authors

*nicolas.lepoul@univ-brest.fr

*ijabin@ulb.ac.be

*olivia.reinaud@parisdescartes.fr

Present Address

#A.G.P.-G.: Laboratoire PHENIX, CNRS UMR 8234, Université Pierre et Marie Curie, 4 place Jussieu, 75252 Paris Cedex 5, France

Notes

The authors declare no competing financial interest.

ACKNOWLEDGMENTS

This work was supported by the Fonds de la Recherche Scientifique-FNRS (FRFC 2.4.617.10.F Project and G.D.L. Ph.D. grant), the Agence Nationale de la Recherche (ANR10-BLAN-714 Cavityzyme(Cu) Project), and the De Brouckère-Solvay and Michel Kaisin funds (G.D.L. travel grants) and was undertaken within the framework of the COST Action CM-1005 “Supramolecular Chemistry in Water”.

REFERENCES

- (1) Yang, H.; Yuan, B.; Zhang, X.; Scherman, O. A. *Acc. Chem. Res.* **2014**, *47* (7), 2106–2115.
- (2) Dong, Z.; Luo, Q.; Liu, J. *Chem. Soc. Rev.* **2012**, *41*, 7890–7908.
- (3) Nimse, S. B.; Kim, T. *Chem. Soc. Rev.* **2013**, *42* (1), 366–386.
- (4) (a) Zhou, J.; Chen, M.; Diao, G. *ACS Appl. Mater. Interfaces* **2013**, *5* (3), 828–836. (b) Zheng, G.; Chen, M.; Liu, X.; Zhou, J.; Xie, J.; Diao, G. *Electrochim. Acta* **2014**, *136*, 301–309. (c) Zhang, S.; Echegoyen, L. *Org. Lett.* **2004**, *6* (5), 791–794. (d) Zhang, S.; Cardona, C. M.; Echegoyen, L. *Chem. Commun.* **2006**, *43*, 4461–4473. (e) Vaze, V. D.; Srivastava, A. K. *Electrochim. Acta* **2007**, *53* (4), 1713–1721.
- (6) (a) Alodhayb, A.; Saydur Rahman, S. M.; Rahman, S.; Valluru, G. K.; Georghiou, P. E.; Beaulieu, L. Y. *Sens. Actuators, B* **2014**, *203*, 766–773. (b) Nakaji-Hirabayashi, T.; Endo, H.; Kawasaki, H.; Gemmei-ide, M.; Kitano, H. *Environ. Sci. Technol.* **2005**, *39*, 5414–5420. (c) Zhang, S.; Palkar, A.; Echegoyen, L. *Langmuir* **2006**, *22*, 10732–10738. (d) Genorio, B.; He, T.; Meden, A.; Polanc, S.; Jamnik, J.; Tour, J. M. *Langmuir* **2008**, *24* (20), 11523–11532. (e) Cormode, D. P.; Evans, A. J.; Davis, J. J.; Beer, P. D. *Dalton Trans.* **2010**, *39* (28), 6532–6541.
- (7) Boccia, A.; Lanzilotto, V.; Zannoni, R.; Pescatori, L.; Arduini, A.; Secchi, A. *Phys. Chem. Chem. Phys.* **2011**, *13* (10), 4444–4451.
- (8) (a) Genorio, B.; Strmcnik, D.; Subbaraman, R.; Tripkovic, D.; Karapetrov, G.; Stamenkovic, V. R.; Pejovnik, S.; Markovic, N. M. *Nat. Mater.* **2010**, *9* (12), 998–1003. (b) Siurdyban, E.; Brotin, T.; Heuze, K.; Vellutini, L.; Buffeteau, T. *Langmuir* **2014**, *30* (49), 14859–14867. (c) Pulkkinen, P. M. S.; Hassinen, J.; Ras, R. H. A.; Tenhu, H. *RSC Adv.* **2014**, *4* (26), 13453–13460. (d) Mendez-Ardoy, A.; Steentjes, T.; Kudernac, T.; Huskens, J. *Langmuir* **2014**, *30* (12), 3467–3476. (e) Ma, X.; Xue, Y.; Dai, L.; Urbas, A.; Li, Q. *Eur. J. Inorg. Chem.* **2013**, *14*, 2682–2686. (f) Domi, Y.; Ikeura, K.; Okamura, K.; Shimazu, K.; Porter, M. D. *Langmuir* **2011**, *27* (17), 10580–10586. (g) Dubacheva, G. V.; Van der Heyden, A.; Dumy, P.; Kaftan, O.; Auzely-Velty, R.; Coche-Guerente, L.; Labbe, P. *Langmuir* **2010**, *26* (17), 13976–13986. (h) Ha, J. M.; Solovyov, A.; Katz, A. *Langmuir* **2009**, *25* (18), 10548–10553. (i) Campiña, J. M.; Martins, A.; Silva, F. *Electrochim. Acta* **2009**, *55* (1), 90–103.
- (9) Le Poul, N.; Le Mest, Y.; Jabin, I.; Reinaud, O. *Acc. Chem. Res.* **2015**, *48* (7), 2097–2106.
- (10) Sénéque, O.; Rager, M.-N.; Giorgi, M.; Reinaud, O. *J. Am. Chem. Soc.* **2000**, *122* (26), 6183–6189.
- (11) Bistri, O.; Colasson, B.; Reinaud, O. *Chem. Sci.* **2012**, *3* (3), 811–818.
- (12) Brunetti, E.; Inthasot, A.; Keymeulen, F.; Reinaud, O.; Jabin, I.; Bartik, K. *Org. Biomol. Chem.* **2015**, *13* (10), 2931–2938.
- (13) Jabin, I.; Reinaud, O. *J. Org. Chem.* **2003**, *68* (9), 3416–3419.
- (14) Izzet, G.; Douziech, B.; Prangé, T.; Tomas, A.; Jabin, I.; Le Mest, Y.; Reinaud, O. *Proc. Natl. Acad. Sci. U. S. A.* **2005**, *102* (19), 6831–6836.
- (15) (a) Gomila, A.; Le Poul, N.; Cosquer, N.; Kerbaol, J. M.; Noel, J. M.; Reddy, M. T.; Jabin, I.; Reinaud, O.; Conan, F.; Le Mest, Y. *Dalton Trans.* **2010**, *39* (48), 11516–11518. (b) Orain, C.; Le Poul, N.; Gomila, A.; Kerbaol, J. M.; Cosquer, N.; Reinaud, O.; Conan, F.; Le Mest, Y. *Chem. - Eur. J.* **2012**, *18* (2), 594–602.
- (16) Orain, C.; Le Poul, P.; Le Mest, Y.; Le Poul, N. *J. Electroanal. Chem.* **2013**, *710*, 48–58.
- (17) Orain, C.; Porrás-Gutiérrez, A. G.; Evoung Evoung, F.; Charles, C.; Cosquer, N.; Gomila, A.; Conan, F.; Le Mest, Y.; Le Poul, N. *Electrochem. Commun.* **2013**, *34*, 204–207.
- (18) (a) Games, L. M.; Hites, R. A. *Anal. Chem.* **1977**, *49* (9), 1433–1440. (b) Grate, J. W. *Chem. Rev.* **2008**, *108* (2), 726–745. (c) Ellis, D. L.; Zakin, M. R.; Bernstein, L. S.; Rubner, M. F. *Anal. Chem.* **1996**, *68* (5), 817–822. (d) Röck, F.; Barsan, N.; Weimar, U. *Chem. Rev.* **2008**, *108* (2), 705–725. (e) Wang, J.; Wang, G.; Ansari, G. A. S.; Khan, M. F. *Toxicol. Appl. Pharmacol.* **2008**, *230* (2), 227–234.
- (19) (a) Finlay, J. A.; Callow, M. E. *Biofouling* **1996**, *9* (4), 257–268. (b) Finlay, J. A.; Callow, M. E. *Biofouling* **1997**, *11* (1), 19–30. (c) Christie, A. O.; Crisp, D. J. *Comp. Biochem. Physiol.* **1966**, *18* (1), 59–69. (d) Christie, A. O.; Crisp, D. J. *J. Appl. Chem.* **1967**, *17* (1), 11–14. (e) Greim, H.; Bury, D.; Klimisch, H. J.; Oeben-Negele, M.; Ziegler-Skylakakis, K. *Chemosphere* **1998**, *36* (2), 271–295. (f) Gagnaire, F.; Azim, S.; Bonnet, P.; Simon, P.; Guenier, J. P.; De Ceaurriz, J. *J. Appl. Toxicol.* **1989**, *9* (5), 301–304. (g) Ngim, K. K.; Ebeler, S. E.; Lew, M. E.; Crosby, D. G.; Wong, J. W. *J. Agric. Food Chem.* **2000**, *48* (8), 3311–3316.
- (20) Lascaux, A.; Delahousse, G.; Ghostin, J.; Bouillon, J.-P.; Jabin, I. *Eur. J. Org. Chem.* **2011**, *27*, 5272–5278.
- (21) Darbost, U.; Rager, M.-N.; Petit, S.; Jabin, I.; Reinaud, O. *J. Am. Chem. Soc.* **2005**, *127* (23), 8517–8525.
- (22) Collman, J. P.; Devaraj, N. K.; Eberspacher, T. P.; Chidsey, C. E. *Langmuir* **2006**, *22* (6), 2457–2464.
- (23) (a) Hohman, J. N.; Thomas, J. C.; Zhao, Y.; Auluck, H.; Kim, M.; Visselaar, W.; Kommeren, S.; Terfort, A.; Weiss, P. S. *J. Am. Chem. Soc.* **2014**, *136* (22), 8110–8121. (b) Saavedra, H. M.; Barbu, C. M.; Dameron, A. A.; Mullen, T. J.; Crespi, V. H.; Weiss, P. S. *J. Am. Chem. Soc.* **2007**, *129* (35), 10741–10746.
- (24) Lhenry, S.; Leroux, Y. R.; Orain, C.; Conan, F.; Cosquer, N.; Le Poul, N.; Reinaud, O.; Le Mest, Y.; Hapiot, P. *Langmuir* **2014**, *30* (15), 4501–4508.
- (25) (a) Rorabacher, D. B. *Chem. Rev.* **2004**, *104* (2), 651–97. (b) Amatore, C.; Barbe, J.-M.; Bucher, C.; Duval, E.; Guillard, R.; Verpeaux, J.-N. *Inorg. Chim. Acta* **2003**, *356*, 267–278. (c) Le Poul, N.; Campion, M.; Izzet, G.; Douziech, B.; Reinaud, O.; Le Mest, Y. *J. Am. Chem. Soc.* **2005**, *127* (15), 5280–5281. (d) Le Poul, N.; Campion, M.; Douziech, B.; Rondelez, Y.; Le Clainche, L.; Reinaud, O.; Le Mest, Y. *J. Am. Chem. Soc.* **2007**, *129* (28), 8801–8810.
- (26) Laviron, E. *J. Electroanal. Chem. Interfacial Electrochem.* **1974**, *52* (3), 395–402.
- (27) Creager, S. E.; Rowe, G. K. *J. Electroanal. Chem.* **1997**, *420* (1–2), 291–299.
- (28) (a) Su, X. J.; Gao, M.; Jiao, L.; Liao, R. Z.; Siegbahn, P. E.; Cheng, J. P.; Zhang, M. T. *Angew. Chem., Int. Ed.* **2015**, *54* (16), 4909–4914. (b) Thorseth, M. A.; Letko, C. S.; Rauchfuss, T. B.; Gewirth, A. A. *Inorg. Chem.* **2011**, *50* (13), 6158–6162. (c) Zhang, J.; Anson, F. C. *J. Electroanal. Chem.* **1992**, *341* (1–2), 323–341.

- (29) Sénèque, O.; Rager, M.-N.; Giorgi, M.; Reinaud, O. *J. Am. Chem. Soc.* **2000**, *122* (26), 6183–6189.
- (30) Rondelez, Y.; Duprat, A.; Reinaud, O. *J. Am. Chem. Soc.* **2002**, *124* (7), 1334–1340.
- (31) Le Poul, N.; Douziech, B.; Zeitouny, J.; Thiabaud, G.; Colas, H.; Conan, F.; Cosquer, N.; Jabin, I.; Lagrost, C.; Hapiot, P.; Reinaud, O.; Le Mest, Y. *J. Am. Chem. Soc.* **2009**, *131* (49), 17800–17807.
- (32) Lide, D. R. *CRC Handbook of Chemistry and Physics*, 84th ed.; CRC Press: Boca Raton, 2003; p 2620.
- (33) Hall, H. K. *J. Am. Chem. Soc.* **1957**, *79* (20), 5441–5444.
- (34) Ramon, G.; Davies, K.; Nassimbeni, L. R. *CrystEngComm* **2014**, *16* (26), 5802–5810.
- (35) Frassinetti, C.; Alderighi, L.; Gans, P.; Sabatini, A.; Vacca, A.; Ghelli, S. *Anal. Bioanal. Chem.* **2003**, *376* (7), 1041–1052.
- (36) Mattiuzzi, A.; Jabin, I.; Mangeney, C.; Roux, C.; Reinaud, O.; Santos, L.; Bergamini, J. F.; Hapiot, P.; Lagrost, C. *Nat. Commun.* **2012**, *3*, 1130–1138.
- (37) Santos, L.; Mattiuzzi, A.; Jabin, I.; Vandencastele, N.; Reniers, F.; Reinaud, O.; Hapiot, P.; Lhenry, S.; Leroux, Y.; Lagrost, C. *J. Phys. Chem. C* **2014**, *118* (29), 15919–15928.
- (38) Noel, J. M.; Sjoberg, B.; Marsac, R.; Zigah, D.; Bergamini, J. F.; Wang, A.; Rigaut, S.; Hapiot, P.; Lagrost, C. *Langmuir* **2009**, *25* (21), 12742–12749.
- (39) Coquière, D.; Le Gac, S.; Darbost, U.; Sénèque, O.; Jabin, I.; Reinaud, O. *Org. Biomol. Chem.* **2009**, *7* (12), 2485–2500.
- (40) Rebillay, J.-N.; Colasson, B.; Bistri, O.; Over, D.; Reinaud, O. *Chem. Soc. Rev.* **2015**, *44* (2), 467–489.
- (41) (a) Izzet, G.; Zeng, X.; Over, D.; Douziech, B.; Zeitouny, J.; Giorgi, M.; Jabin, I.; Le Mest, Y.; Reinaud, O. *Inorg. Chem.* **2007**, *46* (2), 375–377. (b) Izzet, G.; Zeng, X.; Akdas, H.; Marrot, J.; Reinaud, O. *Chem. Commun.* **2007**, *8*, 810–812.
- (42) Sénèque, O.; Campion, M.; Giorgi, M.; Le Mest, Y.; Reinaud, O. *Eur. J. Inorg. Chem.* **2004**, *9*, 1817–1826.
- (43) (a) Coquiere, D.; de la Lande, A.; Marti, S.; Parisel, O.; Prange, T.; Reinaud, O. *Proc. Natl. Acad. Sci. U. S. A.* **2009**, *106* (26), 10449–10454. (b) Coquière, D.; de la Lande, A.; Parisel, O.; Prangé, T.; Reinaud, O. *Chem. - Eur. J.* **2009**, *15* (44), 11912–11917. (c) Lejeune, M.; Picron, J.-F.; Mattiuzzi, A.; Lascaux, A.; De Cesco, S.; Brugnara, A.; Thiabaud, G.; Darbost, U.; Coquière, D.; Colasson, B.; Reinaud, O.; Jabin, I. *J. Org. Chem.* **2012**, *77* (8), 3838–3845.
- (44) Bringmann, G.; Gampe, C. M.; Reichert, Y.; Bruhn, T.; Faber, J. H.; Mikyna, M.; Reichert, M.; Leippe, M.; Brun, R.; Gelhaus, C. *J. Med. Chem.* **2007**, *50* (24), 6104–6115.
- (45) Holtschmidt, V. H.; Oertel, G. *Angew. Makromol. Chem.* **1969**, *9* (1), 1–15.